JOURNAL OF SOLID STATE CHEMISTRY **141,** 70–77 (1998)
ARTICLE NO. SC987917

Preparation and Characterization of Al_2O_3–TiO_2 Composite Oxide Nanocrystals

Gang Xiong, Xin Wang,[1] Lude Lu, Xujie Yang, and Yongfeng Xu

Materials Chemistry Laboratory, Nanjing University of Science and Technology, Nanjing 210094, People's Republic of China

Received January 27, 1998; in revised form April 23, 1998; accepted June 5, 1998

Al_2O_3–TiO_2 composite oxide nanocrystals with different Al_2O_3/TiO_2 ratios (1/4, 2/3, 3/2, and 4/1) were prepared by the poly(ethylene glycol) (PEG) sol–gel method. The preparation process was monitored by thermogravimetric analysis and differential scanning calorimetry (TGA–DSC). Nanocrystal particles of these composite oxides obtained at various heat-treating temperatures (400–1100°C) were characterized in terms of morphology, size, specific surface area, composition, and structure by transmission electron microscopy (TEM), BET specific surface area analysis, and X-ray powder diffractometry (XRD). Nanoparticles of Al_2O_3–TiO_2 with grain sizes in the range 1–150 nm and specific surface areas of 4.3–136 m^2/g could be obtained under different conditions. The morphology of the particles changed from spherical to cubic with increasing heat-treatment temperature. Anatase was stabilized in these composite nanomaterials and the mechanism was discussed. The change of the particles specific surface areas with increase of the Al_2O_3/TiO_2 ratio was researched. The Al_2O_3–TiO_2 composite oxide nanocrystals could catalyze the polymerization of maleic anhydride and may provide a route to obtain a product without rings at the end groups.

***Key Words*: nanocrystal; Al_2O_3–TiO_2; characterization; catalysis.**

INTRODUCTION

More and more attention is being paid to composites of submicrometer particles. This is because the intimate mixing of different phases produces a fine grain size which is resistant to coarsening at elevated temperatures—a necessary condition for superplasticity. Recently, this effect has been exploited in the superplastic forming of Al_2O_3–TiO_2. These kinds of composite oxide have potentially high thermal shock resistance, good flaw tolerance, and appropriate mechanical strength and are thought of highly by material scientists (1, 2). Moreover, they are known to show high catalytic activity for NO_x decomposition removal and oxidation of carbon monoxide, ammonia, methane, and other hydrocarbons and thus could be used as a catalyst for automobile exhaust, waste gas purification, and other chemical reactions.

These materials have been prepared by conventional methods through a solid-state route by firing mixtures of oxides. The products frequently have compositional inhomogeneities and large particles. To obtain homogeneous fine powders, various solution-route preparation methods have been used (3–10). Among these methods are techniques based on using simple organic compounds or organic polymers as a gelling or complexing agent. Kim *et al.* (11) prepared submicrometer, monosized ceramic powders of aluminum titanate, mullite, and the composites of aluminum titanate and mullite by stepwise alkoxide hydrolysis of tetraethylorthosilicate and titanium tetraethoxide in Al_2O_3 ethanolic solution. Low *et al.* (12), using an infiltration technique, prepared functionally gradient Al_2O_3–TiO_2 composites consisting of an alumina host. Mani *et al.* (13) prepared Al_2O_3–TiO_2 powders through thermal decomposition of a transparent gel formed from a mixture of titanium butoxide and boehmite sol in an acetic acid–butanol medium. By using this method, they obtained Al_2O_3–TiO_2 powders with average particle sizes of 2.7 μm at 900°C and 6.5 μm at 1400°C. However, there are currently few papers dealing with the preparation of Al_2O_3–TiO_2 composite oxide nanocrystallines.

In this paper, we report a sol–gel method using poly(ethylene glycol) (PEG) as a gelling agent for the preparation of Al_2O_3–TiO_2 composite oxide nanocrystals. The final products are characterized in terms of particle size, morphology, specific surface area, crystalline structure, and composition. The mechanism of the phase transformation of the products is discussed. The change of the specific surface areas of the products with increasing Al/Ti ratio in the raw materials also is researched. In addition, we have tentatively investigated the catalysis of these composite oxide nanocrystals on the polymerization of maleic anhydride.

[1]To whom correspondence should be addressed.

0022-4596/98 $25.00

EXPERIMENTAL

Sample Preparation

$Ti(SO_4)_2$, $Al(NO_3)_3 \cdot 9H_2O$, and NaOH were of analytical grade. Poly(ethylene glycol) (average molecular weight = 20,000) was used as a starting material without further purification. $Ti(NO_3)_4$ was prepared from $Ti(SO_4)_2$. The procedure for preparing Al_2O_3–TiO_2 composite oxide nanocrystals is schematically illustrated in Fig. 1.

PEG–metal nitrate precursor with a nominal Al_2O_3/TiO_2 ratio equal to 1/4 was prepared as follows: First, stoichiometric amounts of $Al(NO_3)_3$ solution were added to the $Ti(NO_3)_4$ solution. PEG was then added to the mixed solution so that the molar ratio of the PEG repeating unit to the total metal ion content was 3. The PEG–metal nitrate solution was heated at 70–90°C for 4 h with mechanical stirring to evaporate excess water. As the water evaporated, the solution become viscous and finally formed a clear gel.

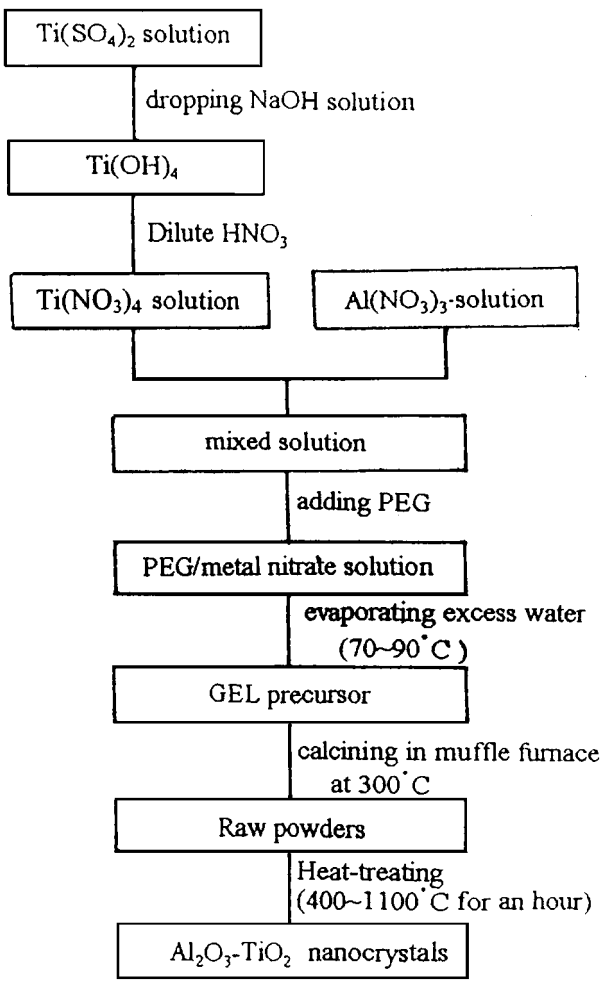

FIG. 1. Flow chart for the preparation of Al_2O_3–TiO_2 composite oxide nanocrystals.

The dried precursor was then placed in a muffle furnace to calcine at 300°C. The precursor gel automatically ignited and 20 min later raw powder was obtained. Further heat-treating the raw powder at various temperatures (400–1100°C) for an hour formed a series of Al_2O_3–TiO_2 composite oxide nanocrystals with different crystalline phases and different particle sizes.

The Al_2O_3–TiO_2 nanoparticles thus obtained are denoted A_1, A_2, A_3, A_4, A_5, A_6, A_7, and A_8. Here 1–8 refer to the heat-treating temperature—400, 500, 600, 700, 800, 900, 1000, and 1100°C, respectively. Products with Al_2O_3/TiO_2 ratios equal to 2/3, 3/2, and 4/1 were prepared through the same procedure and are denoted B_1–B_8, C_1–C_8, and D_1–D_8, respectively.

Characterization

The thermal decomposition in air of the gels during heating was examined by differential scanning calorimetry (DSC) and thermogravimetric analysis (TGA) (Shimadzu DSC–TGA -50 thermal analyzer, heating rate of 10°C/min). X-ray powder diffraction patterns of the particles obtained at temperatures between 400 and 1100°C were taken with a Rigaku D/MAX–III X-ray powder diffractometer operating at 40 kV and using Cu$K\alpha$ radiation not only to characterize the phases of the obtained powders but also to investigate the structure evolution during the heat-treatment process. The specific surface areas were measured by the Brunauer–Emmett–Teller (BET) method at liquid nitrogen temperature using N_2 gas as the adsorbent and samples were degassed at 300°C for 6 h prior to analysis. Transmission electron micrographs (TEM) were taken with a JEM-200CX microscope operating at 15 kV.

Catalysis on the Polymerization of Maleic Anhydride

N,*N*-Dimethylformamide (DMF; 80 ml) and maleic anhydride monomer (27 g) were placed into a three-neck, 200-ml flask. After the maleic anhydride monomer dissolved in the DMF, 0.2 g of catalyst (Al_2O_3–TiO_2 composite oxide nanocrystals with an Al_2O_3/TiO_2 ratio equal to 1/4) was added to the flask and mechanically stirred to ensure complete dispersion in the solution. After 15 min of boiling, the mixture turned brown. Light brown powders were obtained after the mixture had reacted at this temperature for 6 h. The DMF solvent was then evaporated by using an infrared dryer. The infrared absorption spectra of the monomer and the product were obtained on by a Bruker Vector22 Fourier transform infrared (FTIR) spectroscope.

RESULTS AND DISCUSSION

Characterization

Figures 2a–d are the TGA–DSC curves of the gels with different Al/Ti molar ratios. It can be seen that the curves of

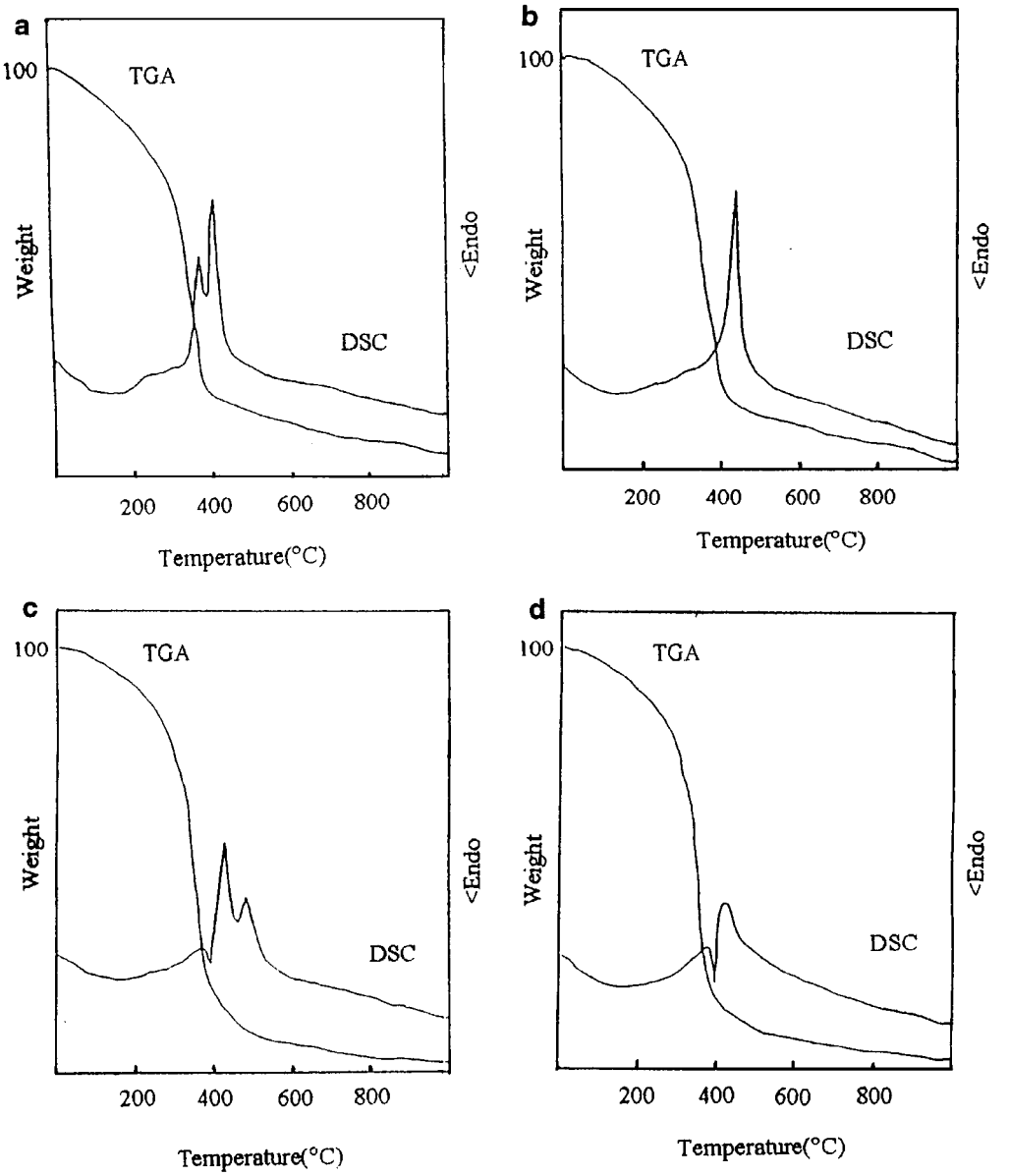

FIG. 2. TGA–DSC curves of the gels: (a) $Al_2O_3/TiO_2 = 1/4$; (b) $Al_2O_3/TiO_2 = 2/3$; (c) $Al_2O_3/TiO_2 = 3/2$; (d) $Al_2O_3/TiO_2 = 4/1$.

all four gels have a broad endothermic peak at about 100°C, accompanied by a weight loss. The weight loss associated with the evaporation of surface water and the melting of the gel. At about 350–480°C, there are one, two, or three exothermic peaks with a relatively large weight loss. As the melting point of poly(ethylene glycol) (PEG) is 65°C and the thermal analysis was performed at a heating rate of 10°C/min with a 10-mg sample, we can infer that the gels had completely melted and the surface water had evaporated when the temperature was increased to 350°C. Thus it can be concluded that there are no endothermic peaks imposed on these exothermic peaks. These peaks are caused by the burning of the organic substances and nitrates or nitro compounds. No further weight loss appears thereafter. This indicates that all of the organics have been burned out. Comparing the TGA–DSC curves of these four gels, we can see that the number and shape of their exothermic peaks in the range 350–480°C are different. There is only a single peak in the gel of sample B ($Al_2O_3/TiO_2 = 2/3$), but two continuous exothermic peaks in sample A ($Al_2O_3/TiO_2 = 1/4$) and sample D ($Al_2O_3/TiO_2 = 4/1$) and three continuous exothermic peaks in sample C ($Al_2O_3/TiO_2 = 3/2$). As we know, PEG was used to enhance the homogeneous mixing of the metal cations. Since PEG has ether oxygens in

its chain, it can interact with metal ions (14). The interaction and the random arrangement of the polymer chain make the metal cations mixed at the molecular level. With the changing of the Al/Ti ratio, the interaction of metal cation with the ether oxygens in the chain of PEG also changes and thus causes the different thermal behaviors of these gels.

The phase compositions of Al_2O_3–TiO_2 composite oxide nanocrystals obtained under different conditions Al/Ti ratios and heat-treatment temperatures) were determined from XRD patterns. The results are listed in Table 1. From Table 1 it can be seen that anatase formed in samples A_1 and B_1 (heat-treated at 400°C), whereas samples C_1 and D_1 were amorphous. All four samples showed anatase when heat-treated at 700°C. No crystallized Al_2O_3 phase formed in any of the four composites when heat-treated at 400, 500, 600, or 700°C. When the heat-treatment temperature was increased to 800°C, γ-Al_2O_3 appeared in all of the samples and transformed to δ-Al_2O_3 at 900°C. Aluminum titanate formed in samples A_6 and B_6 (heat-treated at 900°C) and in samples C_7 and D_7 (heat-treated at 1000°C). The phase compositions are the same for the four samples obtained by heat treatment at 1100°C (samples A_9, B_9, C_9, and D_9). They all had anatase, Al_2TiO_5, δ-Al_2O_3, and α-Al_2O_3, only differing in the ratios of these crystal components caused by the different Al/Ti ratios in the raw materials. It should be noted that anatase transforms completely to rutile at 900°C in pure and bulk TiO_2, but no rutile appeared in the Al_2O_3–TiO_2 composite oxide nanocrystals obtained by the PEG method when the heat-treatment temperature was increased to 1100°C.

TABLE 1
XRD Analysis Results of the Al_2O_3–TiO_2 Composite Oxide Nanocrystals

Heat-treating temperature (°C)	Al_2O_3/TiO_2 ratio	Crystalline phase of sample
400	A_1: $Al_2O_3/TiO_2 = 1/4$	Anatase
	B_1: $Al_2O_3/TiO_2 = 2/3$	Anatase
	C_1: $Al_2O_3/TiO_2 = 3/2$	Amorphous
	D_1: $Al_2O_3/TiO_2 = 4/1$	Amorphous
500	A_2: $Al_2O_3/TiO_2 = 1/4$	Anatase
	B_2: $Al_2O_3/TiO_2 = 2/3$	Anatase
	C_2: $Al_2O_3/TiO_2 = 3/2$	Amorphous
	D_2: $Al_2O_3/TiO_2 = 4/1$	Amorphous
600	A_3: $Al_2O_3/TiO_2 = 1/4$	Anatase
	B_3: $Al_2O_3/TiO_2 = 2/3$	Anatase
	C_3: $Al_2O_3/TiO_2 = 3/2$	Amorphous
	D_3: $Al_2O_3/TiO_2 = 4/1$	Amorphous
700	A_4: $Al_2O_3/TiO_2 = 1/4$	Anatase
	B_4: $Al_2O_3/TiO_2 = 2/3$	Anatase
	C_4: $Al_2O_3/TiO_2 = 3/2$	Anatase
	D_4: $Al_2O_3/TiO_2 = 4/1$	Anatase
800	A_5: $Al_2O_3/TiO_2 = 1/4$	Anatase, γ-Al_2O_3
	B_5: $Al_2O_3/TiO_2 = 2/3$	Anatase, γ-Al_2O_3
	C_5: $Al_2O_3/TiO_2 = 3/2$	Anatase, γ-Al_2O_3
	D_5: $Al_2O_3/TiO_2 = 4/1$	Anatase, γ-Al_2O_3
900	A_6: $Al_2O_3/TiO_2 = 1/4$	Anatase, Al_2TiO_5, δ-Al_2O_3
	B_6: $Al_2O_3/TiO_2 = 2/3$	Anatase, Al_2TiO_5, δ-Al_2O_3
	C_6: $Al_2O_3/TiO_2 = 3/2$	Anatase, δ-Al_2O_3
	D_6: $Al_2O_3/TiO_2 = 4/1$	Anatase, δ-Al_2O_3
1000	A_7: $Al_2O_3/TiO_2 = 1/4$	Anatase, Al_2TiO_5, δ-Al_2O_3
	B_7: $Al_2O_3/TiO_2 = 2/3$	Anatase, Al_2TiO_5, δ-Al_2O_3, α-Al_2O_3
	C_7: $Al_2O_3/TiO_2 = 3/2$	anatase, Al_2TiO_5, δ-Al_2O_3, α-Al_2O_3
	D_7: $Al_2O_3/TiO_2 = 4/1$	Anatase, Al_2TiO_5, δ-Al_2O_3
1100	A_8: $Al_2O_3/TiO_2 = 1/4$	Anatase, Al_2TiO_5, δ-Al_2O_3, α-Al_2O_3
	B_8: $Al_2O_3/TiO_2 = 2/3$	Anatase, Al_2TiO_5, δ-Al_2O_3, α-Al_2O_3
	C_8: $Al_2O_3/TiO_2 = 3/2$	Anatase, Al_2TiO_5, δ-Al_2O_3, α-Al_2O_3
	D_8: $Al_2O_3/TiO_2 = 4/1$	Anatase, Al_2TiO_5, δ-Al_2O_3, α-Al_2O_3

The foregoing experimental results may mainly be caused by the Al^{3+} partially or wholly coming into the space of the TiO_2 lattice and occupying O^{2-} sites. Highly dispersed Al_2O_3 retards interface spreading of the phase transformation process and slows down the nucleation rate of the anatase. With the increase of the Al/Ti ratio, this effect increased, so samples C_1 and D_1 were amorphous whereas samples A_1 and B_1 formed anatase. When the heat-treatment temperature reached 700°C and anatase formed in all four samples, this effect prevented anatase from changing to rutile and still no rutile appeared in all four samples, even at 1100°C. The formation of the Al_2O_3 crystalline phase also is deferred for the same reason.

As with other complex oxides ($ZnFe_2O_4$ and $BaTiO_3$, for example), commercial Al_2TiO_5 powders have traditionally been prepared by the ceramic process, namely calcining the oxide or carbonate precursors of Al and Ti. High calcination temperatures ($\geq$ 1100°C) are needed for the reaction to occur. In the sol–gel process, the precursors are well distributed in the organic gelling agents and thus the temperature of the solid-state reaction could obviously be lowered.

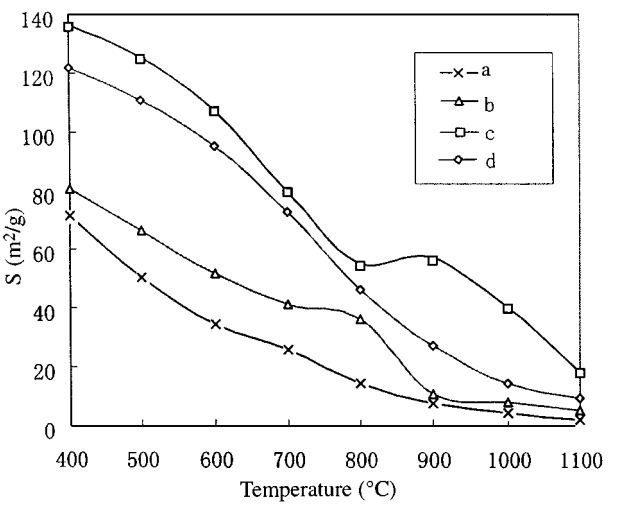

FIG. 3. BET specific surface areas of Al_2O_3–TiO_2 composite oxide nanocrystals: (a) $Al_2O_3/TiO_2 = 1/4$; (b) $Al_2O_3/TiO_2 = 2/3$; (c) $Al_2O_3/TiO_2 = 3/2$; (d) $Al_2O_3/TiO_2 = 4/1$.

Many kinds of complex oxides have been synthesized by the sol–gel technique (15–17) at a temperature lower than that of the ceramic process. In the present experiment, Al_2TiO_5 also formed at temperatures lower than 1100°C (900°C for samples A_6 and B_6 and 1000°C for samples C_7 and D_7).

The specific surface areas of Al_2O_3–TiO_2 composite oxide nanocrystal particles formed under different conditions

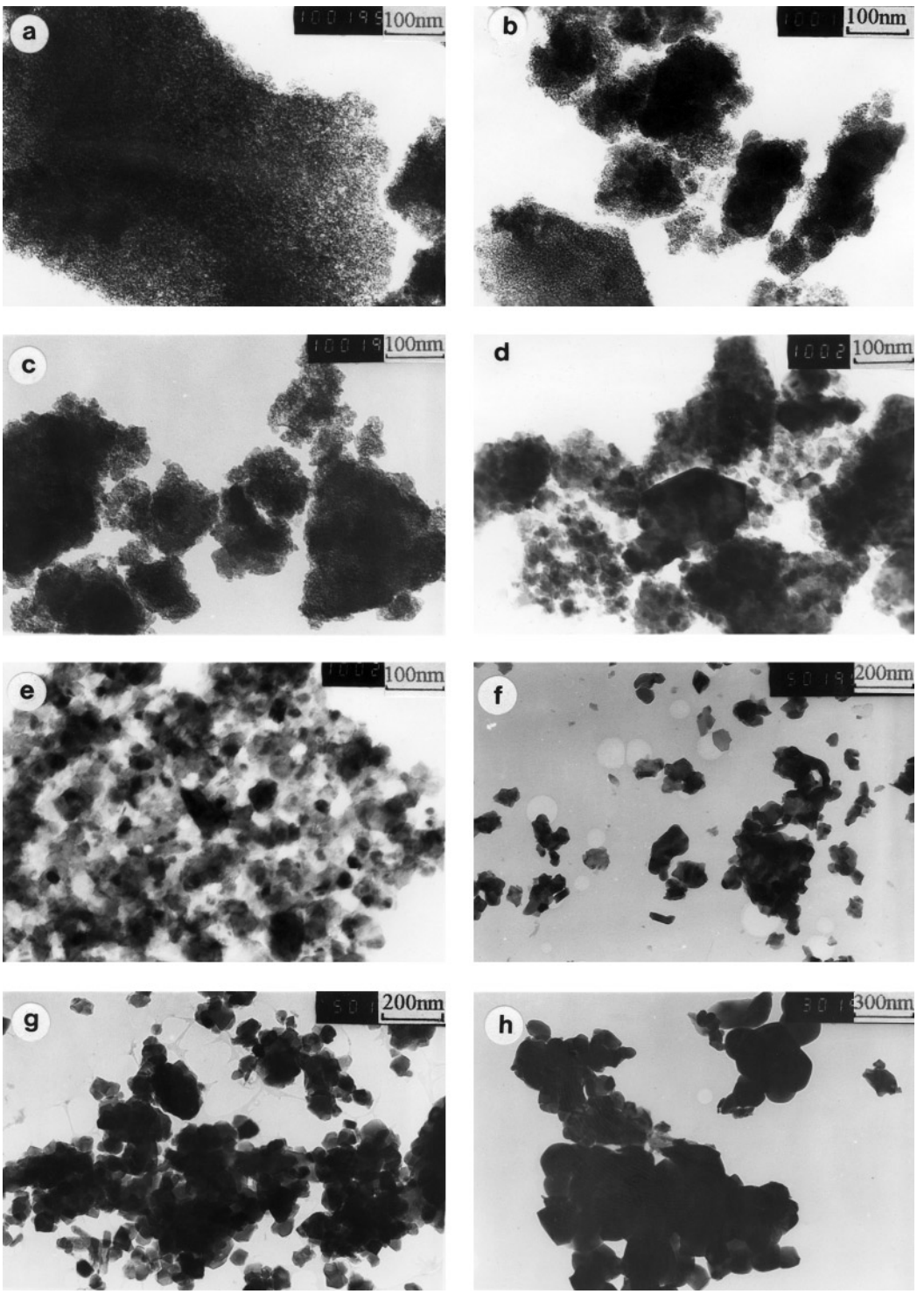

FIG. 4. Morphology of Al_2O_3–TiO_2 composite oxide nanocrystals ($Al_2O_3/TiO_2 = 3/2$) heat-treated at different temperatures: (a) 400°C; (b) 500°C; (c) 600°C; (d) 700°C; (e) 800°C; (f) 900°C; (g) 1000°C; (h) 1100°C.

were determined to investigate the influence of the Al/Ti ratio and the heat-treatment temperature on the sintering properties of Al_2O_3–TiO_2 nanocrystals. The results are illustrated in Fig. 3. It can be seen that with increasing Al/Ti ratio, the specific surface areas increase. This is also caused by the interaction of Al_2O_3 and TiO_2 ultrafine particles. With the Al^{3+} coming into the space of the titania lattice and occupying the O^{2-} site, the volume diffusion resistance of Ti^{4+} and O^{2-} increases and the growing of the particles is retarded. When the Al_2O_3/TiO_2 ratio is equal to 3/2, the product has the best sintering property and the highest specific surface area. With further increase in the

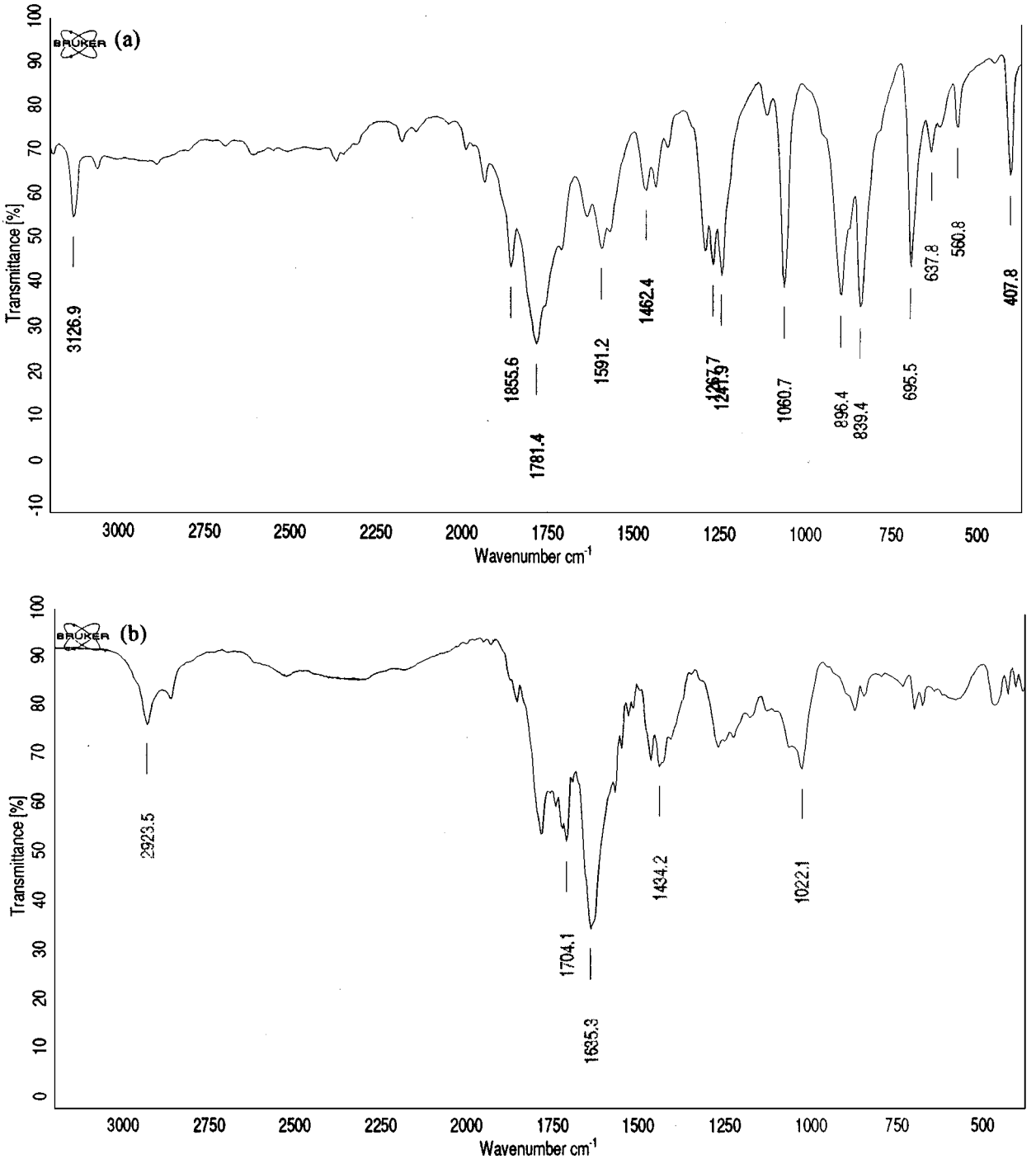

FIG. 5. FTIR spectra of maleic anhydride monomer and the polymerization product: (a) maleic anhydride (b) polymerization product.

Al_2O_3–TiO_2 ratio (4/1), the specific surface areas of the Al_2O_3-TiO_2 composite oxide particles decrease. This may mainly be caused by the amassing of the Al_2O_3 particles in the composite and thus a decrease in the intimate mixing of Al_2O_3 and TiO_2 fine particles. On the other hand, the specific surface areas of all the samples decreased with the increase of heat-treatment temperature. The result is consistent with the law of sintering of ceramic particles.

The morphology of the Al_2O_3–TiO_2 composite oxide nanocrystals (samples C_1–C_8) is shown in Fig. 4. It can be seen from Fig. 4 that the particles obtained at 400°C are spherical and of uniform size, with grain sizes are in the range 1–4 nm. With increasing heat-treatment temperature, the particle size increases gradually, and the morphology changes from spherical to cubic.

For spherical particles the specific surface area is related to the particle size D through the density ρ: $S = 6/(\rho D)$. According to this equation, the average particle size of sample C_1 can be calculated. It is found to be 12.4 nm, which is inconsistent with the TEM data. This is believed to be the result of agglomeration of the nanosized powders owing to the high surface energy of the ultrafine particles. The adsorptive capacity of N_2 decreased with gathering of the powders and the specific surface area thus determined is smaller than the actual value, so the particle size calculated through the foregoing equation is larger (17).

Catalysis on the Polymerization of Maleic Anhydride

The Fourier transform infrared absorption spectra of the maleic anhydride monomer and the product after reaction are shown in Figs 5a and 5b. In the spectra of maleic anhydride, the band at 3126 cm^{-1} was assigned to the vibration of the C–H bond of the double bond (C=C), the bands at 1855, 1760, and 1781 cm^{-1} were due to the absorption of the carbonyl group, the bands at 1242 and 896 cm^{-1} were assigned to the vibration absorption of the C–O–C bond, and the bands at 1591, 839, and 695 cm^{-1} were ascribed to the vibration of the double bond. The FTIR spectrum of the product shown in Fig. 5b indicates that the strong absorption band at 695 cm^{-1} greatly decreased and the band at 3126 cm^{-1} disappeared. The band at 2923 cm^{-1} was attributed to the stretching vibration of the C–H bond of $–CH_2–$. These changes show that the maleic anhydride monomer had polymerized by using the Al_2O_3–TiO_2 composite oxide nanocrystals ($Al_2O_3/TiO_2 = 1/4$) as a catalyst. The result tentatively indicates that these composite nanomaterials have an excellent catalysis effect on the polymerization of maleic anhydride. Traditionally, the polymerization of maleic anhydride has been initiated by using benzoyl peroxide (BPO) or pyridine as an initiating agent (18–20). The polymerization products thus prepared have rings at the end groups. To obtain a more useful product, researchers have intensively sought for a method to synthesize poly(maleic anhydride) without rings at the end groups but still have not made much progress. The investigation results presented in this paper provide a possible way to solve this problem. Further research on the catalysis mechanism and properties of the polymerization product is still under way and will be reported elsewhere.

CONCLUSIONS

1. Al_2O_3–TiO_2 composite oxide nanocrystals were prepared by a sol–gel process using PEG as a gelling agent. An Al_2TiO_5 crystalline phase formed in these composites at heat-treatment temperatures above 1000°C.
2. Highly dispersed Al_2O_3 can slow down the nucleation rate of TiO_2 and stabilize anatase. No rutile phase appeared in any of these samples.
3. The proportion of the components of Al_2O_3–TiO_2 composite nanocrystals has great influence on their properties. With change of the Al/Ti ratio, the thermal decomposition behaviors of the gels, the conditions for crystalline phase transformation, and the specific surface areas show obvious differences. When the Al_2O_3/TiO_2 ratio is equal to 3/2, the composite oxide particles have the highest specific surface areas. With the increasing heat-treatment temperature, the shape of the composite oxide nanoparticles changes from spherical to cubic and the specific surface area decreases.
4. The Al_2O_3–TiO_2 composite oxide nanocrystals have an excellent catalysis effect on the polymerization of maleic anhydride.

ACKNOWLEDGMENTS

This project was supported by the Doctoral Foundation of the National Committee of Education of China and the Foundation of Natural Science of Jiangsu province.

REFERENCES

1. H. Morishima, Z. Kato, K. Uemtsu, K. Saito, T. Yano, and N. Ootsuka, *J. Am. Ceram. Soc.* **69,** C226 (1986).
2. J. J. Cleveland and R. C. Bradt, *J. Am. Ceram. Soc.* **61,** 478 (1978).
3. H. Morishima, Z. Kato, K. Uemtsu, K. Saito, T. Yano, and N. Ootsuka, *J. Mater. Sci. Lett.* **6,** 389 (1987).
4. T. E. Klimova and J. R. Solis, *Mater. Sci. Forum.* **152–153**, 309 (1994).
5. J. A. Montoya, J. M. Dominguez, T. Viveros, D. Chadwick, and K. Zheng, *J. Sol–Gel Sci. Technol.* **2,** 431 (1994).
6. T. Klimova, Y. Huerta, M. L. R. Cervantes, R. M. M. Aranda and Z. Martin, *J. Stud. Surf. Sci. Catal.* **91,** 411 (1995).
7. T. Viveros, A. Zarate, M. A. Lopez, J. A. Montoya, R. Ruiz, and M. Portilla, *J. Stud. Surf. Sci. Catal.* **91,** 807 (1995).
8. J. Ramirez, T. Klimova, Y. Huerta, and J. Aracil, *Appl. Catal., A* **118,** 73 (1994).
9. Kumar and Krishnankutty-Nair, *Appl. Catal., A* **119,** 163 (1994).
10. H. A. J. Thomas and R. Stevens, *Br. Ceram. Proc.* **42,** 117 (1989).

11. I. J. Kim, C. Zografou, and W. Kroenert, *Int. J. Mater. Prod. Technol.* **8,** 440 (1993).
12. I. M. Low, R. D. Skala, and D. Zhou, *J. Mater. Sci. Lett*., **15,** 345 (1996).
13. T. Y. Mani, H. K. Varma, K. C. Warrier, and A. D. Damodaran, *J. Am. Ceram. Soc*. **74,** 1807 (1991).
14. T. Okada, *Analyst* **118,** 959 (1993).
15. X. Li and H. B. Zhang, *J. Mater. Chem.* **2,** 253 (1992).
16. T. Fukui, C. Sakurai, and M. Okuyama, *J. Mater. Sci.* **32,** 189 (1997).
17. G. Xiong, Z. L. Zhi, X. J. Yang, L. D. Lu, and X. Wang, *J. Mater. Sci*., *Lett*. **16,** 1064 (1997).
18. J. L. Lang and W. A. Pavelich, *J. Polym. Sci*., *Part A* **1,** 1123 (1963).
19. W. Regel and C. Schneider, *Macromol. Chem. Phys.* **182,** 237 (1981).
20. R. Bacskai, *J. Polym. Sci.* **14,** 1797 (1976).